

## Correspondence Relations for Fracture Parameters of Interface Corners in Anisotropic Viscoelastic Materials

Chyanbin Hwu<sup>1</sup>, Tai-Liang Kuo<sup>2</sup>

**Abstract:** The problems of the interface corners between two dissimilar anisotropic viscoelastic materials are studied in this paper. Through the use of the well-known correspondence principle between linear elasticity and linear viscoelasticity, fracture parameters in the Laplace domain can be obtained from the path-independent H-integral for the corresponding problems of anisotropic linear elastic materials. Further application of the correspondence relations for fracture parameters proposed in our recent study then leads us the solutions of fracture parameters in the time domain. To show the applicability and accuracy of the proposed method, several different kinds of numerical examples are presented such as a centered interface crack, free edges between two dissimilar materials, and the interface corners appeared within the electronic packages. The fracture parameters calculated in this study include the orders of stress singularity and the stress intensity factors of opening mode, shearing mode and tearing mode. The proposed method allows the orders of stress singularity be real or complex, repeated or distinct, and the fracture mode be pure mode or mixed mode.

**Keywords:** Correspondence principle, path-independent H-integral, interface corners, stress singularity, stress intensity factors.

### 1 Introduction

In engineering applications, most of polymeric materials are treated as viscoelastic materials which exhibit a time and rate dependence. To promote the development of new materials for modern industries, considerable attention has been devoted to the investigation of the materials which possess anisotropic viscoelastic properties [Volkov (2005); Selovanov (2010)]. To deal with the two-dimensional problems of anisotropic viscoelasticity and piezoelectricity, a special boundary element for

---

<sup>1</sup> Institute of Aeronautics and Astronautics, National Cheng Kung University, Taiwan, ROC.

<sup>2</sup> Material and Chemical Research Laboratories, Industrial Technology Research Institute, Taiwan, ROC.

anisotropic piezoelectric and viscoelastic solids containing interfaces/holes/cracks/inclusions was developed [Chen and Hwu (2010); Chen and Hwu (2011)], and an extended Stroh formalism for anisotropic viscoelasticity was established [Kuo and Hwu (2013)].

Many important works had been devoted to develop the computing technique for the stress intensity factors of cracked body, such as the SGBEM-based methods [Dong and Atluri (2013)] and the multipole dual boundary element method [Wang and Yao (2011)]. However, comparatively few studies were presented to calculate the stress intensity factors of a body containing the corner surrounded by many different materials. The interface corners are structural configurations appearing commonly within macro- or micro- engineering objects. Cracks in homogeneous materials and interface cracks between two dissimilar materials are special cases of interface corners by adjusting the corner angles and material properties to the required conditions. Thus, a unified approach studying the problems of interface corners is a connecting bridge for the understanding of fracture behavior of materials [Hwu and Kuo (2007); Hwu, Kuo, and Chen (2009)].

If the boundary of a viscoelastic body is invariant with time, the correspondence principle is generally employed to obtain the viscoelastic solutions from the corresponding elastic solutions [Christensen (1982)]. In our recent study, the correspondence relations for fracture parameters of interface corners in anisotropic viscoelastic materials have been proposed and justified through the comparison of four different calculating approaches [Kuo and Hwu (2013)]. In that study, the approach employing the proposed correspondence relations for fracture parameters together with the use of path-independent H-integral was proved to be the most efficient and accurate one. To extend the applicability of the proposed correspondence relations, further discussions are provided in this paper on the repetition of orders of stress singularity and the application to the common problems appeared in the electronic packages. To avoid the complex expressions involved in the present problem, the matrix form near tip solutions of interface corners proposed in [Hwu (2012)] were utilized.

## 2 Linear Anisotropic Viscoelasticity

In a fixed rectangular coordinate system  $x_i, i = 1, 2, 3$ , let  $u_i$ ,  $\sigma_{ij}$ , and  $\varepsilon_{ij}$  be, respectively, the displacement, stress and strain. The constitutive laws for the linear anisotropic viscoelastic materials, the strain-displacement relations for the small deformations, and the equilibrium equations for static loading conditions can be written as [Haddad (1995)]

$$\begin{aligned}\sigma_{ij}(t) &= C_{ijkl}(t)\varepsilon_{kl}(0) + \int_0^t C_{ijkl}(t-\tau) \frac{\partial \varepsilon_{kl}(\tau)}{\partial \tau} d\tau, \\ \varepsilon_{ij}(t) &= \frac{1}{2} \{ u_{i,j}(t) + u_{j,i}(t) \}, \quad \sigma_{ij,j}(t) = 0,\end{aligned}\tag{1}$$

where  $i, j, k, l = 1, 2, 3$ , and the repeated indices imply summation; a subscript comma stands for differentiation;  $C_{ijkl}(t)$  is the elastic stiffness tensor whose components are also known to be the *relaxation functions* of the viscoelastic materials, and the symmetry of stress and strain imply  $C_{ijkl}(t) = C_{jikl}(t) = C_{ijlk}(t)$ . Taking the Laplace transform of Eq. 1 gives

$$\check{\sigma}_{ij}(s) = s\check{C}_{ijkl}(s)\check{\varepsilon}_{kl}(s), \quad \check{\varepsilon}_{ij}(s) = \frac{1}{2} \left\{ \check{u}_{i,j}(s) + \check{u}_{j,i}(s) \right\}, \quad \check{\sigma}_{ij,j}(s) = 0, \quad (2)$$

where  $s$  is the transform variable and the Laplace transform  $\check{f}(s)$  of  $f(t)$  is defined as

$$\check{f}(s) = \int_0^\infty f(t) e^{-st} dt. \quad (3)$$

Equations (2) are identical to the basic equations of linear anisotropic elasticity. Thus, if the boundary of a viscoelastic body is invariant with time, the viscoelastic solutions in the Laplace domain can be obtained directly from the solutions of the corresponding elastic problems by replacing the elastic stiffness tensor  $C_{ijkl}$  with  $s\check{C}_{ijkl}(s)$ . This statement is the so-called *correspondence principle* between linear elasticity and linear viscoelasticity and is applicable to anisotropic viscoelastic materials.

By applying the correspondence principle and the Stroh formalism for two-dimensional linear anisotropic elasticity [Ting (1996); Hwu (2010)], the general solutions satisfying the 15 partial differential equations, Eq. 2, can be written as

$$\check{\mathbf{u}}(\mathbf{x}, s) = 2\operatorname{Re}\{\mathbf{A}_s(s)\mathbf{f}_s(z, s)\}, \quad \check{\boldsymbol{\phi}}(\mathbf{x}, s) = 2\operatorname{Re}\{\mathbf{B}_s(s)\mathbf{f}_s(z, s)\}, \quad (4a)$$

where

$$\check{\mathbf{u}} = \begin{Bmatrix} \check{u}_1 \\ \check{u}_2 \\ \check{u}_3 \end{Bmatrix}, \quad \check{\boldsymbol{\phi}} = \begin{Bmatrix} \check{\phi}_1 \\ \check{\phi}_2 \\ \check{\phi}_3 \end{Bmatrix}, \quad \mathbf{f}_s(z, s) = \begin{Bmatrix} f_1^s(z_1, s) \\ f_2^s(z_2, s) \\ f_3^s(z_3, s) \end{Bmatrix}, \quad (4b)$$

$$\mathbf{A}_s(s) = [\mathbf{a}_1^s(s) \quad \mathbf{a}_2^s(s) \quad \mathbf{a}_3^s(s)], \quad \mathbf{B}_s(s) = [\mathbf{b}_1^s(s) \quad \mathbf{b}_2^s(s) \quad \mathbf{b}_3^s(s)],$$

$$z_k = x_1 + \mu_k^s x_2, \quad k = 1, 2, 3.$$

$\check{\mathbf{u}}$  and  $\check{\boldsymbol{\phi}}$  are the displacement and stress function vectors in the Laplace domain, and  $\check{\phi}_i$  is related to the stresses in the Laplace domain by

$$\check{\sigma}_{i1} = -\check{\phi}_{i,2}, \quad \check{\sigma}_{i2} = \check{\phi}_{i,1}. \quad (5)$$

$\mathbf{f}_s(z, s)$  is a function vector composed of three holomorphic complex functions  $f_\alpha^s(z_\alpha, s)$ ,  $\alpha = 1, 2, 3$ .  $\mu_\alpha^s$  and  $(\mathbf{a}_\alpha^s, \mathbf{b}_\alpha^s)$  are the material eigenvalues and eigenvectors in the Laplace domain. In [Kuo and Hwu (2013)],  $\mu_\alpha^s$  were proved to be independent of the transform variable  $s$  for the standard linear viscoelastic solids, and moreover, the explicit solutions of  $\mathbf{A}_s(s)$  and  $\mathbf{B}_s(s)$  for isotropic linear viscoelastic solids were also derived.

### 3 Fracture Parameters in the Laplace Domain

Consider an interface corner between two dissimilar anisotropic viscoelastic materials (Fig. 1), in which perfect bond is assumed along the interface. Through the use of correspondence principle and the matrix power function form solution for the corresponding elastic problems, the near tip solution in the Laplace domain can be expressed as [Hwu (2012)]

$$\check{\boldsymbol{\sigma}}(r, \theta, s) = \frac{1}{\sqrt{2\pi\ell}}(r/\ell)^{-\Delta_s(\theta, s)} \mathbf{k}_s(\theta, s), \quad (6)$$

where  $(r, \theta)$  is a local polar coordinate with origin at the corner tip, and  $s$  is the transform variable of the Laplace domain;  $\ell$  is a reference length which may be chosen arbitrarily;  $\check{\boldsymbol{\sigma}}(r, \theta, s)$  is a stress vector composed of the traction along  $\theta = \text{constant}$ , i.e.,

$$\check{\boldsymbol{\sigma}}(r, \theta, s) = \begin{Bmatrix} \sigma_{r\theta}(r, \theta, s) \\ \sigma_{\theta\theta}(r, \theta, s) \\ \sigma_{\theta 3}(r, \theta, s) \end{Bmatrix}. \quad (7)$$

$\Delta_s(\theta, s)$  and  $\mathbf{k}_s(\theta, s)$  are the matrix of singular orders and the stress intensity factors  $\mathbf{k}_s(\theta)$  in the Laplace domain, which can be calculated as follows [Hwu (2012)].

#### 3.1 Matrix of singular orders in the Laplace domain

(i) If no matter the singular orders  $\delta_\alpha^s$ ,  $\alpha = 1, 2, 3$ , are real or complex, repeated or distinct, their associated eigenfunctions  $\lambda_\alpha^s(\theta)$ ,  $\alpha = 1, 2, 3$  are independent each other, then

$$\Delta_s(\theta, s) = \mathbf{\Lambda}_s^*(\theta) < \delta_\alpha^s > \mathbf{\Lambda}_s^{*-1}(\theta), \quad \mathbf{\Lambda}_s^*(\theta) = \mathbf{\Omega}(\theta) \mathbf{\Lambda}_s(\theta) \quad (8)$$

where  $\mathbf{\Omega}(\theta)$  and  $\mathbf{\Lambda}_s(\theta)$  are, respectively, the rotation matrix and the matrix of stress eigenfunction defined by

$$\mathbf{\Omega}(\theta) = \begin{bmatrix} \cos \theta & \sin \theta & 0 \\ -\sin \theta & \cos \theta & 0 \\ 0 & 0 & 1 \end{bmatrix}, \quad \mathbf{\Lambda}_s(\theta) = [\boldsymbol{\lambda}_1^s(\theta) \ \boldsymbol{\lambda}_2^s(\theta) \ \boldsymbol{\lambda}_3^s(\theta)]. \quad (9)$$

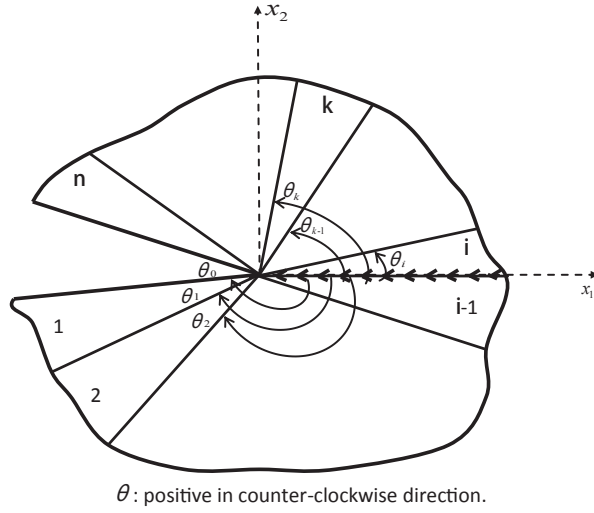


Figure 1: Multi-material wedges.

The angular bracket  $\langle \rangle$  used in Eq. 8 stands for a diagonal matrix in which each component is varied according to the subscript  $\alpha$ , e.g.,  $\langle \delta_\alpha^s \rangle = \text{diag.}[\delta_1^s, \delta_2^s, \delta_3^s]$ .  
(ii) If one of the singular orders  $\delta_\alpha^s, \alpha = 1, 2, 3$ , is a double root and no enough independent eigenfunctions exist, i.e., if  $\delta_1^s = \delta_2^s, \boldsymbol{\lambda}_1^s(\theta) = \boldsymbol{\lambda}_2^s(\theta)$ , then

$$\Delta_s(\theta, s) = \dot{\boldsymbol{\Lambda}}_s^*(\theta) \langle \delta_\alpha^s \rangle \dot{\boldsymbol{\Lambda}}_s^{*-1}(\theta), \quad \dot{\boldsymbol{\Lambda}}_s^*(\theta) = \boldsymbol{\Omega}(\theta) \dot{\boldsymbol{\Lambda}}_s(\theta) \quad (10a)$$

where

$$\dot{\boldsymbol{\Lambda}}_s(\theta) = [\boldsymbol{\lambda}_1^s(\theta) \dot{\boldsymbol{\lambda}}_1^s(\theta) \boldsymbol{\lambda}_3^s(\theta)]. \quad (10b)$$

(iii) If one of the singular orders  $\delta_\alpha^s, \alpha = 1, 2, 3$ , is a triple root and no enough independent eigenfunctions exist, i.e., if  $\delta_1^s = \delta_2^s = \delta_3^s, \boldsymbol{\lambda}_1^s(\theta) = \boldsymbol{\lambda}_2^s(\theta) = \boldsymbol{\lambda}_3^s(\theta)$ , then

$$\Delta_s(\theta, s) = \ddot{\boldsymbol{\Lambda}}_s^*(\theta) \langle \delta_\alpha^s \rangle \ddot{\boldsymbol{\Lambda}}_s^{*-1}(\theta), \quad \ddot{\boldsymbol{\Lambda}}_s^*(\theta) = \boldsymbol{\Omega}(\theta) \ddot{\boldsymbol{\Lambda}}_s(\theta) \quad (11a)$$

where

$$\ddot{\boldsymbol{\Lambda}}_s(\theta) = [\boldsymbol{\lambda}_1^s(\theta) \dot{\boldsymbol{\lambda}}_1^s(\theta) \ddot{\boldsymbol{\lambda}}_1^s(\theta)]. \quad (11b)$$

In the above, the over dot means differentiation with respect to the singular order, i.e.,

$$\dot{\boldsymbol{\lambda}}_1^s(\theta) = \frac{\partial}{\partial \delta_1^s} \{\boldsymbol{\lambda}_1^s(\theta)\}, \quad \ddot{\boldsymbol{\lambda}}_1^s(\theta) = \frac{\partial^2}{\partial \delta_1^s} \{\boldsymbol{\lambda}_1^s(\theta)\}. \quad (12)$$

The symbols with the forms of  $\langle f_\alpha \rangle$  and  $\langle f_\alpha \rangle$  are defined as

$$\langle f_\alpha \rangle = \begin{bmatrix} f_1 & \frac{\partial f_1}{\partial \delta_1^s} & 0 \\ 0 & f_1 & 0 \\ 0 & 0 & f_3 \end{bmatrix}, \quad \langle f_\alpha \rangle = \begin{bmatrix} f_1 & \frac{\partial f_1}{\partial \delta_1^s} & \frac{\partial^2 f_1}{\partial \delta_1^{s2}} \\ 0 & f_1 & 2\frac{\partial f_1}{\partial \delta_1^s} \\ 0 & 0 & f_1 \end{bmatrix}. \quad (13)$$

Therefore,

$$\langle \delta_\alpha^s \rangle = \begin{bmatrix} \delta_1^s & 1 & 0 \\ 0 & \delta_1^s & 0 \\ 0 & 0 & \delta_3^s \end{bmatrix}, \quad \langle \delta_\alpha^s \rangle = \begin{bmatrix} \delta_1^s & 1 & 0 \\ 0 & \delta_1^s & 2 \\ 0 & 0 & \delta_1^s \end{bmatrix}. \quad (14)$$

In matrix operation, it is known that if  $f(\Delta) = \sum_{m=0}^{\infty} c_m \Delta^m$  converges, and if  $\Delta$  is similar to a diagonal matrix, such as  $\Delta = \Lambda^* \langle \delta_\alpha \rangle \Lambda^{*-1}$  shown in Eq. 8, then  $f(\Delta) = \Lambda^* \langle f(\delta_\alpha) \rangle \Lambda^{*-1}$ . With this understanding, the matrix power function  $(r/\ell)^{-\Delta_s(\theta,s)}$  given in Eq. 6 can be calculated by

$$(r/\ell)^{-\Delta_s(\theta,s)} = \begin{cases} \Lambda_s^*(\theta) \langle (r/\ell)^{-\delta_\alpha^s} \rangle \Lambda_s^{*-1}(\theta), & \text{for case (i),} \\ \dot{\Lambda}_s^*(\theta) \langle (r/\ell)^{-\delta_\alpha^s} \rangle \dot{\Lambda}_s^{*-1}(\theta), & \text{for case (ii),} \\ \ddot{\Lambda}_s^*(\theta) \langle (r/\ell)^{-\delta_\alpha^s} \rangle \ddot{\Lambda}_s^{*-1}(\theta), & \text{for case (iii).} \end{cases} \quad (15)$$

In Eqs. 8-15, the singular orders  $\delta_\alpha^s$  and their associated eigenfunctions  $\lambda_\alpha^s(\theta)$ ,  $\alpha = 1, 2, 3$  can be determined from the following eigenrelation [Hwu (2012)]

$$\begin{aligned} \text{bonded : } & (\mathbf{K}_e - \mathbf{I}) \mathbf{w}_0 = \mathbf{0}, \quad \mathbf{w}_0 = (\mathbf{u}_0 \ \boldsymbol{\phi}_0)^T, \\ \text{free-free : } & \mathbf{K}_e^{(3)} \mathbf{u}_0 = \mathbf{0}, \quad \boldsymbol{\phi}_0 = \mathbf{0}, \\ \text{fixed-fixed : } & \mathbf{K}_e^{(2)} \boldsymbol{\phi}_0 = \mathbf{0}, \quad \mathbf{u}_0 = \mathbf{0}, \\ \text{free-fixed : } & \mathbf{K}_e^{(1)} \mathbf{u}_0 = \mathbf{0}, \quad \boldsymbol{\phi}_0 = \mathbf{0}, \\ \text{fixed-free : } & \mathbf{K}_e^{(4)} \boldsymbol{\phi}_0 = \mathbf{0}, \quad \mathbf{u}_0 = \mathbf{0}, \end{aligned} \quad (16)$$

in which  $\mathbf{K}_e^{(i)}$ ,  $i = 1, 2, 3, 4$  are the submatrices of  $\mathbf{K}_e$  defined by

$$\mathbf{K}_e = \begin{bmatrix} \mathbf{K}_e^{(1)} & \mathbf{K}_e^{(2)} \\ \mathbf{K}_e^{(3)} & \mathbf{K}_e^{(4)} \end{bmatrix}, \quad \text{and } \mathbf{K}_e = \mathbf{E}_n \mathbf{E}_{n-1} \dots \mathbf{E}_1. \quad (17)$$

$\mathbf{E}_k = \hat{\mathbf{N}}_k^{1-\delta}(\theta_k, \theta_{k-1})$  is the  $(1-\delta)$ th power of the key matrix  $\hat{\mathbf{N}}_k(\theta_k, \theta_{k-1})$  whose definition can be found in [Hwu, Omiya, and Kishimoto (2003)], and  $\theta_k$ ,  $\theta_{k-1}$  are the angular location of the two sides of the  $k$ th wedge (Fig. 1).

### 3.2 Stress intensity factors in the Laplace domain

From the near tip solution given in Eq. 6, the stress intensity factor in the Laplace domain can be defined as

$$\mathbf{k}_s(\theta, s) = \lim_{r \rightarrow 0} \sqrt{2\pi\ell}(r/\ell)^{\Delta_s(\theta, s)} \check{\boldsymbol{\sigma}}(r, \theta, s). \quad (18)$$

Let  $\mathbf{k}_s(s) = \mathbf{k}_s(0, s)$  and  $\Delta_s(s) = \Delta_s(0, s)$ , with  $\theta = 0$  we have

$$\mathbf{k}_s(s) = \lim_{r \rightarrow 0} \sqrt{2\pi\ell}(r/\ell)^{\Delta_s(s)} \check{\boldsymbol{\sigma}}(r, 0, s). \quad (19)$$

Like the problems of anisotropic elasticity, the stress intensity factors defined in Eq. 19 can be calculated by the path-independent H-integral through the following relation [Hwu and Huang (2012)]

$$\mathbf{k}_s = \begin{Bmatrix} K_{II}^s \\ K_I^s \\ K_{III}^s \end{Bmatrix} = \boldsymbol{\Lambda}_s \mathbf{H}^{*-1} \mathbf{h}, \mathbf{h} = \begin{Bmatrix} H_1 \\ H_2 \\ H_3 \end{Bmatrix}, \quad (20a)$$

where  $\boldsymbol{\Lambda}_s = \boldsymbol{\Lambda}_s(0)$

$$\begin{aligned} \mathbf{H}^* &= \int_{\theta_0}^{\theta_n} [\hat{\boldsymbol{\Lambda}}'_s(\theta) \mathbf{V}_s(\theta) - \hat{\mathbf{V}}_s^T(\theta) \boldsymbol{\Lambda}'_s(\theta)] d\theta, \\ H_k &= \int_{\Gamma} (\check{\mathbf{u}}^T \hat{\mathbf{t}}_k - \hat{\mathbf{u}}_k^T \check{\mathbf{t}}) d\Gamma, k = 1, 2, 3. \end{aligned} \quad (20b)$$

In Eq. 20a,  $K_{II}^s, K_I^s, K_{III}^s$  are functions of  $s$  and are, respectively, the stress intensity factors of shearing mode, opening mode and tearing mode in the Laplace domain. In Eq. 20b, the integral ends  $\theta_0$  and  $\theta_n$  are the angle of corner flanks;  $\boldsymbol{\Lambda}_s(\theta)$  and  $\mathbf{V}_s(\theta)$  are, respectively, the eigenfunction matrices of stresses and displacements; the prime  $\bullet'$  means the derivative with respective to the polar angle  $\theta$ ; the over-hat  $\check{\bullet}$  stands for the values of the auxiliary system; the superscript  $T$  denotes the transpose of a matrix;  $\check{\mathbf{u}}$  and  $\check{\mathbf{t}}$  in the second equation of Eq. 20b are the displacement vector and traction vector of the actual system with the transformed elastic properties  $s\check{C}_{ijkl}(s)$ , which can be obtained using appropriate method, such as finite element, boundary element, or experimental testing, and  $\hat{\mathbf{u}}_k$  and  $\hat{\mathbf{t}}_k$  are those of the auxiliary system which have been obtained in [Hwu and Huang (2012)] as

$$\begin{aligned} \hat{\mathbf{u}}_k(r, \theta, s) &= \frac{\sqrt{2\pi\ell}}{r} \hat{\mathbf{V}}_s(\theta, s) \langle (1 - \delta_\alpha^s)(r/\ell)^{\delta_\alpha^s} \rangle \mathbf{i}_k, \\ \hat{\mathbf{t}}_k(r, \theta, s) &= \frac{\sqrt{2\pi\ell}}{r^2} \hat{\boldsymbol{\Lambda}}'_s(\theta, s) \langle (1 - \delta_\alpha^s)(r/\ell)^{\delta_\alpha^s} \rangle \mathbf{i}_k, \end{aligned} \quad (21a)$$

where

$$\mathbf{i}_1 = \begin{Bmatrix} 1 \\ 0 \\ 0 \end{Bmatrix}, \mathbf{i}_2 = \begin{Bmatrix} 0 \\ 1 \\ 0 \end{Bmatrix}, \mathbf{i}_3 = \begin{Bmatrix} 0 \\ 0 \\ 1 \end{Bmatrix}. \quad (21b)$$

#### 4 Correspondence Relations

If the near tip solutions in the time domain can also be written in the matrix power function form such as Eq. 6, we have

$$\boldsymbol{\sigma}(r, \theta, t) = \frac{1}{\sqrt{2\pi\ell}}(r/\ell)^{-\Delta(\theta,t)} \mathbf{k}(\theta, t) \quad (22)$$

The stress intensity factors  $\mathbf{k}(\theta, t)$  in the time domain can then be defined as

$$\mathbf{k}(\theta, t) = \lim_{r \rightarrow 0} \sqrt{2\pi\ell}(r/\ell)^{\Delta(\theta,t)} \boldsymbol{\sigma}(r, \theta, t). \quad (23)$$

Let  $\mathbf{k}(t) = \mathbf{k}(0, t)$  and  $\Delta(t) = \Delta(0, t)$ , with  $\theta = 0$  we have

$$\mathbf{k}(t) = \lim_{r \rightarrow 0} \sqrt{2\pi\ell}(r/\ell)^{\Delta(t)} \boldsymbol{\sigma}(r, 0, t), \quad (24a)$$

or

$$\begin{Bmatrix} K_{II} \\ K_I \\ K_{III} \end{Bmatrix} = \lim_{r \rightarrow 0} \sqrt{2\pi\ell}(r/\ell)^{\Delta(t)} \begin{Bmatrix} \sigma_{r\theta}(r, \theta, t) \\ \sigma_{\theta\theta}(r, \theta, t) \\ \sigma_{\theta 3}(r, \theta, t) \end{Bmatrix}_{\theta=0}, \quad (24b)$$

where  $K_{II}, K_I, K_{III}$  are, respectively, the stress intensity factors of shearing mode, opening mode and tearing mode in the time domain. By inclusion of the non-singular terms, equating Eq. 22 with the inversion of Eq. 6 leads to

$$\begin{aligned} & (r/\ell)^{-\Delta(t)} \mathbf{k}(t) + \text{nonsingular terms} \\ &= L^{-1}\{(r/\ell)^{-\Delta_s(s)} \mathbf{k}_s(s) + \text{nonsingular terms}\}. \end{aligned} \quad (25)$$

From Eq. 25, the correspondence relations for the singular orders, the eigenfunctions, and the stress intensity factors have been proposed to be [Kuo and Hwu (2013)]

$$s\check{\delta}_\alpha = \delta_\alpha^s, s\check{\Delta} = \Delta_s, s\check{\mathbf{V}} = \mathbf{V}_s, s\check{\Lambda} = \Lambda_s, \check{\mathbf{k}} = \mathbf{k}_s, \quad (26)$$

where  $\mathbf{V} \equiv \mathbf{V}(\theta)$  and  $\Lambda \equiv \Lambda(\theta)$  are eigenfunction matrices of displacements and stress functions in the time domain, and  $\Lambda(\theta)$  is related to the matrix of singular orders  $\Delta(\theta, t)$  by

$$\Delta(\theta, t) = \Lambda^*(\theta) < \delta_\alpha > \Lambda^{*-1}(\theta), \quad \Lambda^*(\theta) = \Omega(\theta)\Lambda(\theta) \quad (27)$$

Using the correspondence relations shown in Eq. 26, the singular orders  $\delta_\alpha$  and the stress intensity factor  $\mathbf{k}$  in the time domain can then be calculated via Laplace inversion as

$$\delta_\alpha(t) = L^{-1}\{\delta_\alpha^s/s\}, \quad \mathbf{k}(t) = L^{-1}\{\mathbf{k}_s(s)\}. \quad (28)$$

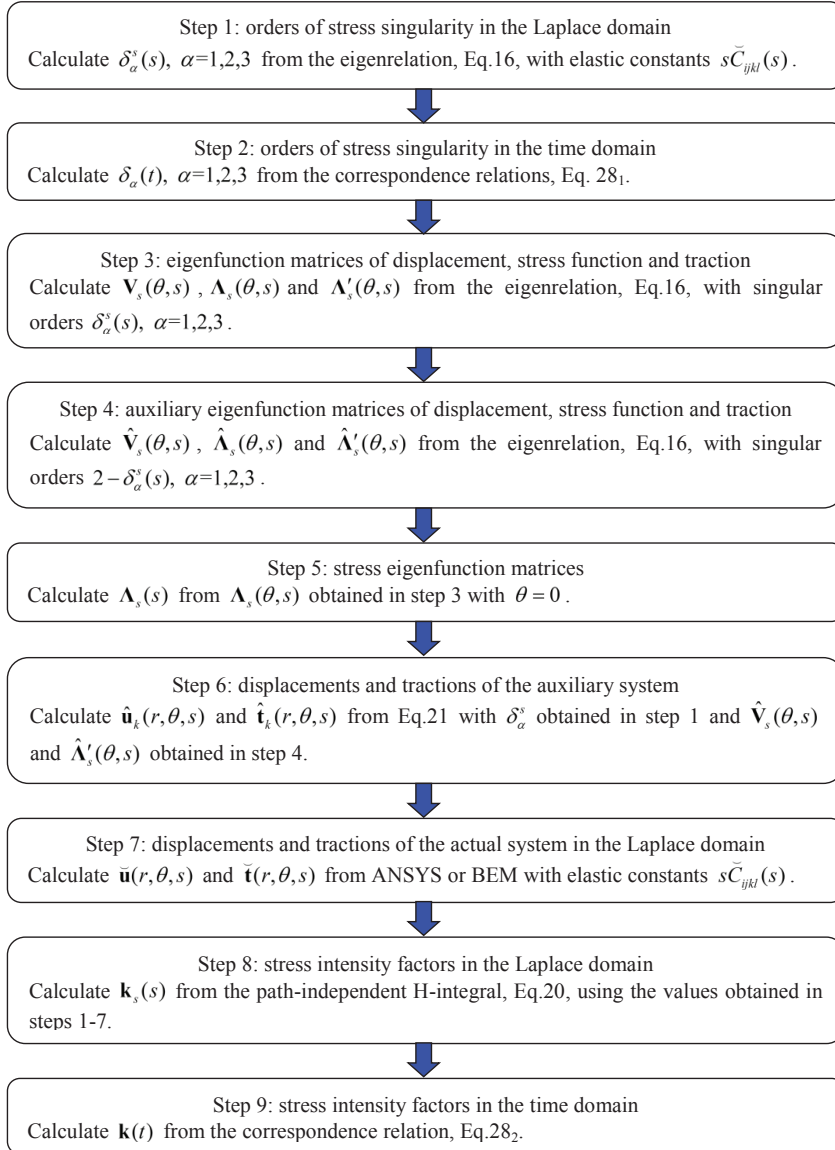


Figure 2: Flow chart for the calculation of stress intensity factors in the time domain.

## 5 Numerical Examples

In [Kuo and Hwu (2013)], the approach, *Laplace domain H-integral with elastic near tip solution*, was suggested for calculating the orders of stress singularity and

the stress intensity factors in the time domain. In this section three examples were analyzed and discussed by following this approach whose calculating procedure is shown in Fig. 2. Note that, in steps 2 and 9, the values of  $\delta_\alpha(t) = L^{-1}\{\delta_\alpha^s(s)\}$  and  $\mathbf{k}(t) = L^{-1}\{\mathbf{k}_s(s)\}$  were obtained through the use of Schapery's collocation method [Schapery (1962)]. Based on the convergent tests, the number of terms in the exponential series of the collocation method is chosen to be 19 and the range of transform variable  $s$  is chosen to be  $10^{-6} \sim 10^6$  to perform all the following examples which include the analyses for the interface cracks, free edges, and interface corners.

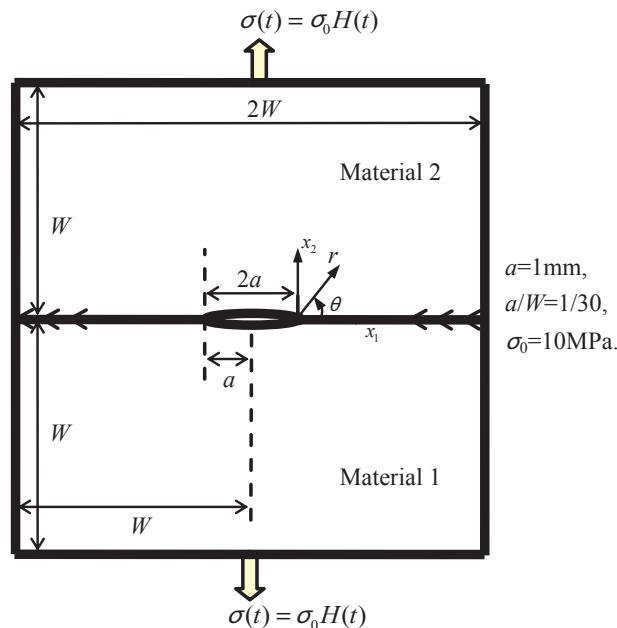


Figure 3: A center interface crack between two dissimilar materials.

### 5.1 Example 1: Interface Cracks

Three cases are discussed in this example, i.e., an interface crack (1) between two dissimilar isotropic viscoelastic materials, (2) between one isotropic viscoelastic material and one isotropic elastic material, and (3) between one orthotropic viscoelastic material and one orthotropic elastic material. The loading and geometry of this example are shown in Fig. 3 in which  $\sigma(t) = \sigma_0 H(t)$  and  $H(t)$  is the Heaviside step function. The material combinations for these three cases are listed in Tab.

1 in which  $G(t)$ ,  $\kappa(t)$ , and  $v(t)$  are, respectively, shear modulus, bulk modulus, and Poisson's ratio measured from the relaxation test;  $\mathbf{C}(t)$  is the  $6 \times 6$  relaxation modulus matrix and  $C_{ij}^0$  and  $C_{ij}^\infty$ ,  $i,j = 1,2,\dots,6$ , are the components of the matrices  $\mathbf{C}^0$  and  $\mathbf{C}^\infty$ ; the superscripts 0 and  $\infty$  denote, respectively, the initial value and terminal value;  $\tau$  is the relaxation time that determines the rate of decay. All the three examples are assumed to be under the generalized plane stress condition.

Table 1: Material combinations for the three cases of example 1.

	material 1	material 2
case 1	$G^0 = 5.807\text{GPa}$ , $G^\infty = 2.652\text{GPa}$ , $G(t) = G^\infty + (G^0 - G^\infty)e^{-t/\tau}$ , $v(t) = 0.3$ , $\tau = 10\text{ sec}$ .	$G^0 = 1.308\text{GPa}$ , $G^\infty = 0.1308\text{GPa}$ $G(t) = G^\infty + (G^0 - G^\infty)e^{-t/\tau}$ , $\kappa(t) = 2.833\text{GPa}$ , $\tau = 0.1\text{ sec}$ .
case 2	Young's modulus: 85GPa Poisson's ratio: 0.2	$G^0 = 1.308\text{GPa}$ , $G^\infty = 0.1308\text{GPa}$ $G(t) = G^\infty + (G^0 - G^\infty)e^{-t/\tau}$ , $\kappa(t) = 2.833\text{GPa}$ , $\tau = 0.1\text{ sec}$ .
case 3	$C_{11} = 23.577\text{GPa}$ , $C_{22} = C_{33} = 22.772\text{GPa}$ , $C_{12} = C_{13} = 7.452\text{GPa}$ , $C_{23} = 8.276\text{GPa}$ , $C_{44} = C_{55} = C_{66} = 4.600\text{GPa}$	$C_{11}^0 = 1.323\text{GPa}$ , $C_{22}^0 = C_{33}^0 = 1.111\text{GPa}$ , $C_{12}^0 = C_{13}^0 = 0.513\text{GPa}$ , $C_{23}^0 = 0.518\text{GPa}$ , $C_{44}^0 = C_{55}^0 = C_{66}^0 = 0.240\text{GPa}$ , $C_{ij}^\infty = 0.5C_{ij}^0$ , $C(t) = C^\infty + (C^0 - C^\infty)e^{-t/\tau}$ $\tau = 0.5\text{ sec}$ .

It's known that the singular order of an interface crack between two dissimilar elastic materials has a general expression as  $0.5, 0.5 \pm i\varepsilon$ , in which  $\varepsilon$  is the so-called *oscillatory index* whose analytical closed-form solution has been given in [Ting (1996)]. Using the correspondence principle, this analytical solution can be extended in the Laplace domain. Then, through the closed-form solution for the singular orders in the Laplace domain and the Schapery's collocation method for Laplace inversion, the numerical results of the singular orders show that  $\delta_\alpha(t) = 0.5, 0.5 \pm i\varepsilon(t)$  whose real part doesn't vary with time while the imaginary part is time-dependent and can be calculated by

$$\varepsilon(t) = L^{-1} \left\{ \frac{1}{2\pi s} \ln \frac{\check{G}_1 + s\check{G}_2\check{\kappa}_1}{\check{G}_2 + s\check{G}_1\check{\kappa}_2} \right\}, \quad \check{\kappa} = \frac{3 - s\check{v}}{s(1 + s\check{v})}, \quad (29a)$$

for the first two cases and

$$\varepsilon(t) = L^{-1} \left\{ \frac{1}{2\pi s} \ln \frac{1+\beta}{1-\beta} \right\}, \quad \beta = \left[ -\frac{1}{2} \text{tr} (\mathbf{WD}^{-1})^2 \right]^{1/2}, \quad (29b)$$

for case 3.

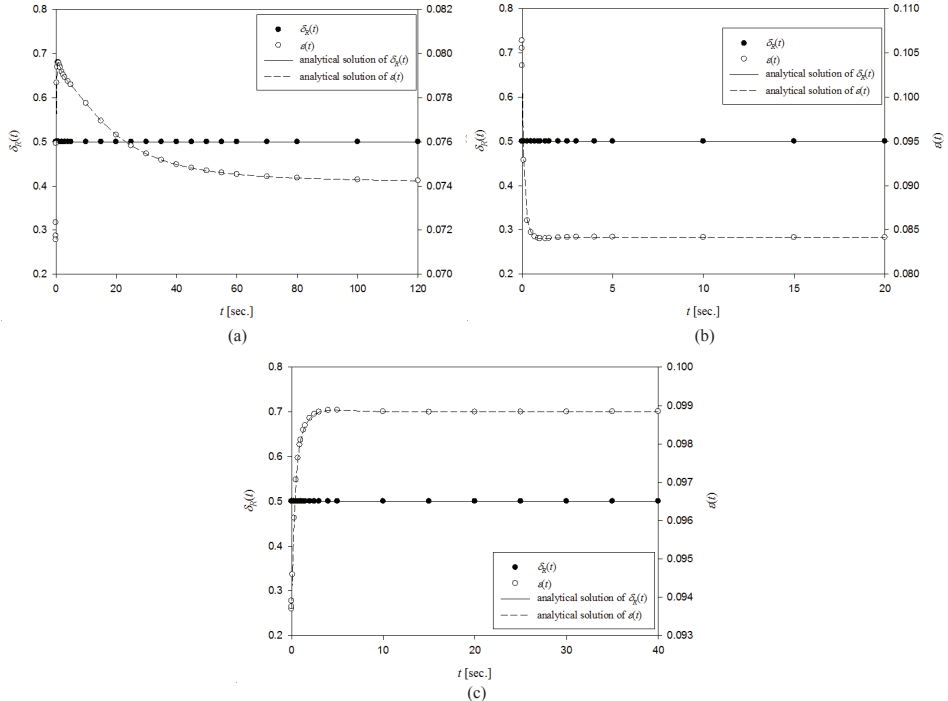


Figure 4: The orders of stress singularity for interface cracks: (a) case 1, (b) case 2, and (c) case 3 of example 1.

In Eq.29a, the subscripts 1 and 2 denote the properties of material 1 and 2, respectively. In Eq.29b, the matrices  $\mathbf{D}$  and  $\mathbf{W}$  are the real and the negative of the imaginary parts of the bimaterial matrix  $\mathbf{M}^*$  [Hwu (1993); Hwu (2010)] whose elastic constants are  $s\bar{C}_{ijkl}(s)$ . The results of  $\delta_\alpha(t) = \delta_R(t) + i\varepsilon(t)$  calculated numerically through the flow chart shown in Fig. 2 and analytically through Eq. 29 are plotted in Figs. 4a, 4b, and 4c which show excellent agreement between analytical and numerical solutions for all three cases.

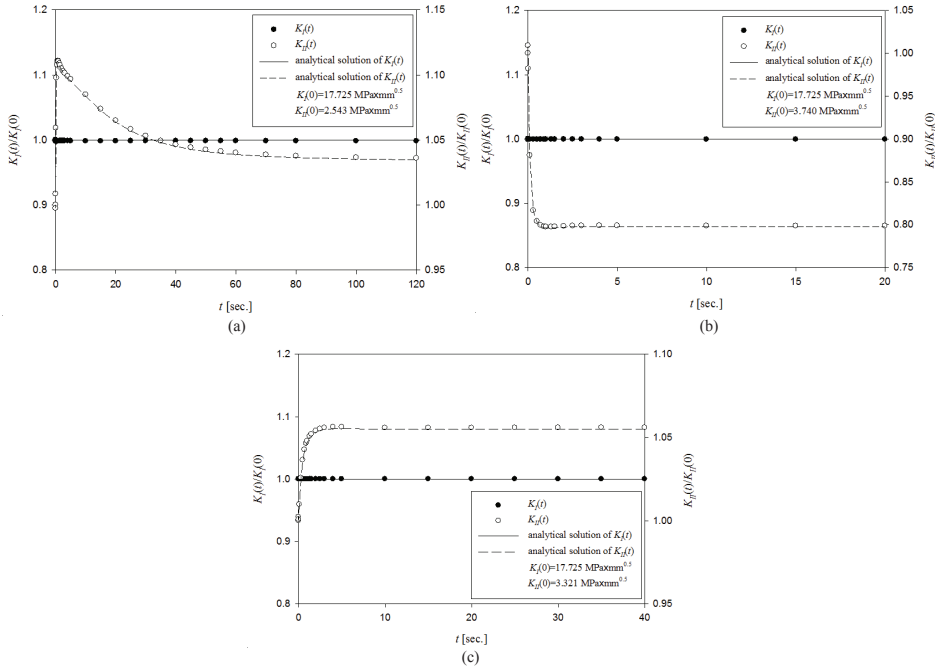


Figure 5: The stress intensity factors for interface cracks: (a) case 1, (b) case 2, and (c) case 3 of example 1.

The numerical results of stress intensity factors are plotted in Figs. 5a, 5b, and 5c in which the analytical solutions are also shown. Note that the analytical solutions were provided in [Kuo and Hwu (2013)] as

$$\begin{aligned} K_I(t) &= L^{-1} \left\{ \frac{\sigma_0}{s} \sqrt{\pi a} \left[ \cos \left( \varepsilon^s \ln \frac{2a}{\ell} \right) - 2\varepsilon^s \sin \left( \varepsilon^s \ln \frac{2a}{\ell} \right) \right] \right\}, \\ K_{II}(t) &= L^{-1} \left\{ -\frac{\sigma_0}{s} \sqrt{\pi a} \left[ \sin \left( \varepsilon^s \ln \frac{2a}{\ell} \right) - 2\varepsilon^s \cos \left( \varepsilon^s \ln \frac{2a}{\ell} \right) \right] \right\}, \end{aligned} \quad (30)$$

where the reference length  $\ell$  is chosen to be  $2a$  in this example. In Figs. 5a, 5b, and 5c, the maximum difference between the numerical results and the analytical solutions Eq.29 is only 0.15% for  $K_{II}(t)$  at 1.3sec. of case 2.

## 5.2 Example 2: Free edges

Consider a bimaterial subjected to a uniform tension  $\sigma(t) = \sigma_0 H(t)$  under the generalized plane strain condition (Fig. 6). The bimaterial is made up of two dissimilar isotropic viscoelastic materials whose properties can be characterized by the shear relaxation function  $G(t)$  and the constant bulk modulus  $\kappa$ . The shear relaxation

function is considered to have the form shown in case 1 of material 2 of Tab. 1. In this example,

$$\begin{aligned} G^0 &= 1.31 \text{ GPa}, G^\infty = 0.13 \text{ GPa}, \tau = 0.1 \text{ sec.}, \kappa = 2.84 \text{ GPa, for material 1,} \\ G^0 &= 5.81 \text{ GPa}, G^\infty = 2.65 \text{ GPa, } \tau = 10 \text{ sec.}, \kappa = 12.59 \text{ GPa, for material 2.} \end{aligned}$$

The point A located on the free edge of Fig. 6 is a special case of interface corners whose corner angles upper and below the interface are both  $\pi/2$ . The reference length  $\ell$  needed for the calculation of the stress intensity factor is selected to be 0.01mm. Figs. 7a and 7b show the results of singular orders and stress intensity factors at point A of free edge. To know the influence of the solution sources of actual system, two different numerical solutions of actual system are used. One is from the finite element software ANSYS using PLANE183 with 4028 elements 12213 nodes, and the other is from a special boundary element (BEM) developed in [Chen and Hwu (2011)] with 80 elements 84 nodes. The results of Fig. 7b show that the stress intensity factors calculated from the actual systems provided by ANSYS and BEM with the transformed elastic properties  $s\bar{C}_{ijkl}(s)$  are close to each other. It is worthy to mention that only one singular order exists as shown in Fig. 7a during the time period of analyses for this example.

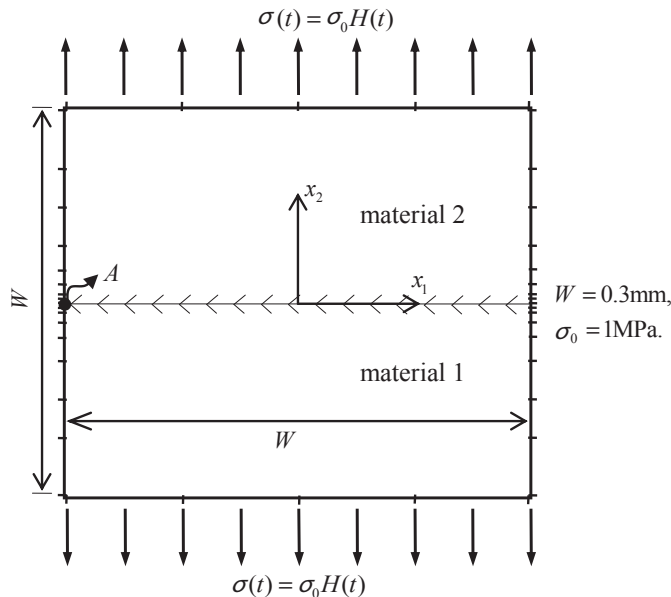


Figure 6: Free edges between two dissimilar viscoelastic materials.

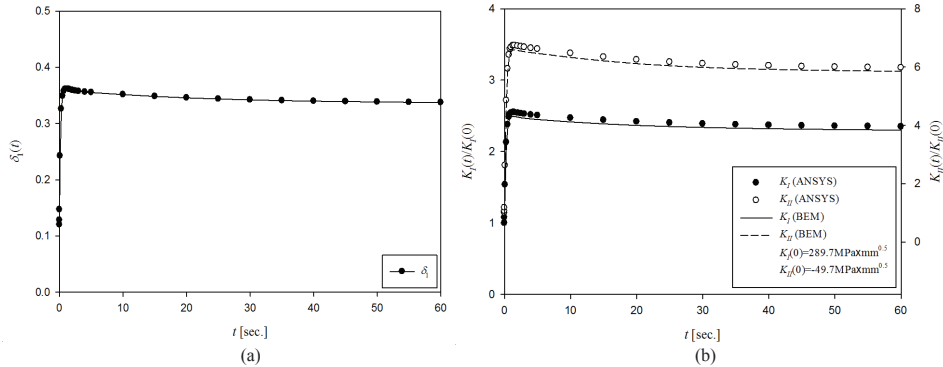


Figure 7: (a) The orders of stress singularity, and (b) the stress intensity factors at point A of free edge of example 2.

### 5.3 Example 3: Interface Corners

To demonstrate the applicability of the proposed method, two representative portions usually appearing within the electronic package are shown (see Figs. 8a and 8b), and the interface corners with tips A and B were analyzed in this example. Both the EMC and the solder ball are assumed to be the viscoelastic materials whose properties are given in case 1 of material 1 of Tab. 1. The FR4-PCB is an orthotropic elastic material whose properties are given in case 3 of material 1 of Tab. 1. The remaining of the electronic package are the silicon die and the BT substrate which are isotropic elastic materials with

Young's modulus=26GPa and Poisson's ratio=0.3 for silicon die,

Young's modulus=22GPa and Poisson's ratio=0.11 for BT substrate.

Generalized plane strain condition is used in this example. Both of these two cases use the reference length  $\ell = 0.3\text{mm}$ . The effect of the angle of corner A on the orders of stress singularity is plotted in Fig. 9 which shows that the larger the opening angle  $\beta$  the smaller the singular order  $\delta(t)$ , while the decay rate of each opening angle only has a little difference. Note that the singular order shown in Fig. 9 is the most critical singular order whose real part is the largest among all the singular orders.

Figures 10 and 11 show the results of singular orders and stress intensity factors at points A whose opening angle of point A is fixed at  $\beta = 135^\circ$ , and point B with opening angle  $68.23^\circ$ . Reasonable time decay is shown in these two figures. Note that point A has two singular orders and point B has three singular orders during the time period of analyses. As stated in Section 3, the proposed method can always be

employed no matter which kinds of singular orders appear in the interface corners.

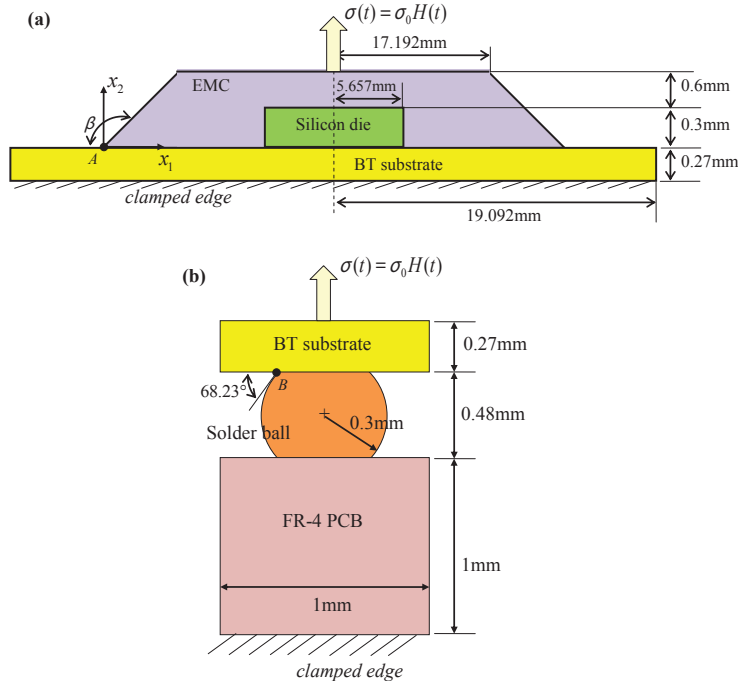


Figure 8: Interface corners within electronic packages: (a) portion 1, and (b) portion 2.

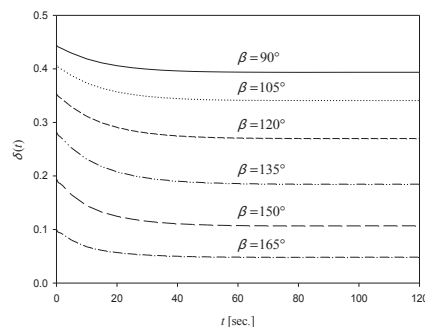


Figure 9: The orders of stress singularity  $\delta(t)$  versus the opening angle  $\beta$  of the interface corner A.

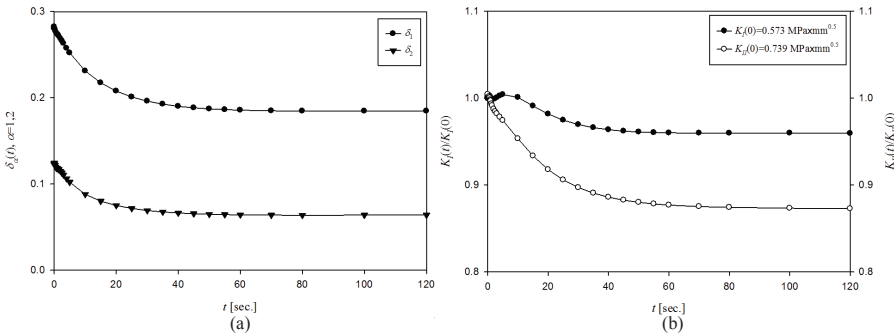


Figure 10: (a) The orders of stress singularity, and (b) the stress intensity factors of the interface corner A of example 3.

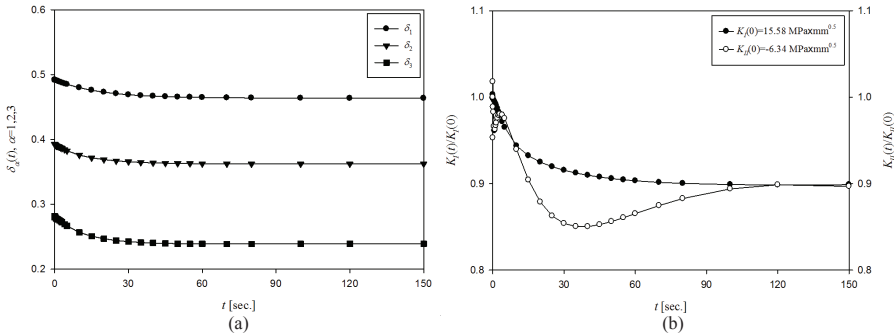


Figure 11: (a) The orders of stress singularity, and (b) the stress intensity factors of the interface corner B of example 3.

## 6 Conclusions

The well-known correspondence principle between linear elasticity and linear viscoelasticity was extended to the relations for fracture parameters of interface corners. According to these correspondence relations, the orders of stress singularity and the stress intensity factors of interface corners in anisotropic viscoelastic materials were calculated in this paper for three different examples: (1) interface cracks between two dissimilar materials, elastic and/or viscoelastic, isotropic or orthotropic, (2) free edges between two dissimilar isotropic viscoelastic materials, (3) interface corners appearing within the electronic package. The results show that the proposed method is accurate and efficient for any kinds of corner angles and material combinations of anisotropic viscoelastic materials. The combination

covers the commonly interested cases of cracks, interface cracks and free edges. The arbitrariness of angles and materials is reflected by the fact that the orders of stress singularity are allowed to be real or complex, repeated or distinct.

### Acknowledgement

The authors would like to thank National Science Council, TAIWAN, R.O.C. for support through Grant NSC 100-2221-E-006102-MY3.

### References

- Chen, Y. C.; Hwu, C.** (2010): Green's Functions for Anisotropic/Piezoelectric Biomaterials and Their Applications to Boundary Element Analysis. *CMES: Computer Modeling in Engineering & Sciences*, vol. 57, no.1, pp. 31-50.
- Chen, Y. C.; Hwu, C.** (2011): Boundary element analysis for viscoelastic solids containing interfaces/holes/cracks/inclusions. *Engineering Analysis with Boundary Element*, vol. 35, pp. 1010-1018
- Christensen, R.M.** (1982): *Theory of Viscoelasticity – an Introduction* Academic Press, New York.
- Dong, L.; Atluri, S. N.** (2013): Fracture & Fatigue Analyses: SGBEM-FEM or XFEM? Part 1: 2D Structures. *CMES: Computer Modeling in Engineering & Sciences*, vol. 90, no.2, pp. 91-146.
- Dong, L.; Atluri, S. N.** (2013). Fracture & Fatigue Analyses: SGBEM-FEM or XFEM? Part 2: 3D solids. *CMES: Computer Modeling in Engineering & Sciences*, vol. 90, no.5, pp. 379-413.
- Hwu, C.** (1993): Fracture parameters for the orthotropic bimaterial interface cracks. *Engineering Fracture Mechanics*, vol. 45, pp. 8997
- Haddad, T. M.** (1995): *Viscoelasticity of Engineering Materials*, Chapman & Hall.
- Hwu, C.; Omiya, M.; Kishimoto, K.** (2003): A key matrix  $\mathbf{N}$  for the stress singularity of the anisotropic elastic composite wedges. *JSME International Journal Series A*, vol. 46, pp. 40-50.
- Hwu, C.; Kuo, T. L.** (2007): A unified definition for stress intensity factors of interface corners and cracks. *International Journal of Solids and Structures*, vol. 44, pp. 6340-6359.
- Hwu, C.; Kuo, T. L.; and Chen, Y. C.** (2009). Interfaces between two dissimilar elastic materials. *CMC: Computers, Materials, & Continua*, vol. 11, no.3, pp. 165-184.
- Hwu, C.** (2010): *Anisotropic Elastic Plates*. Springer, New York.

- Hwu, C.** (2012): Matrix form near tip solutions of interface corners. *International Journal of Fracture*, vol. 176, pp. 1-16.
- Hwu, C.; Huang, H. Y.** (2012): Investigation of the stress intensity factors for interface corners. *Engineering Fracture Mechanics*, vol. 93, pp. 204-224.
- Kuo, T. L.; Hwu, C.** (2013): Interface corners in linear anisotropic viscoelastic materials. *International Journal of Solids and Structures*, vol. 50, pp. 710-724.
- Schapery, R. A.** (1962): Approximate methods of transform inversion for viscoelastic stress analysis. *Proceedings of the 4<sup>th</sup> U.S. National Congress on Applied Mechanics*, pp. 1075-1085.
- Selivanov, M. F.** (2010): Influence of the viscoelastic properties of a composite on the stress distribution around an elliptic hole in a plate. *International Applied Mechanics*, vol. 46, pp. 799-805.
- Ting, T. C. T.** (1996): *Anisotropic Elasticity: Theory and Applications*. Oxford Science Publications, New York.
- Volkov, V. S.** (2005): Relaxation thermodynamics and viscoelasticity of anisotropic polymer systems. *Journal of Engineering Physics and Thermophysics*, vol. 78, pp. 862-870.
- Wang, H. T.; Yao, Z. H.** (2011): A fast multipole dual boundary element method for the three-dimensional crack problems. *CMES: Computer Modeling in Engineering & Sciences*, vol. 72, no.2, pp. 115-147.

